PHILOSOPHICAL TRANSACTIONS OF THE ROYAL SOCIETY B BIOLOGICAL SCIENCES

Heterogeneous Morphology and Tracer Coupling Patterns of Retinal Oligodendrocytes

Edith C. G. M. Hampson and Stephen R. Robinson

Phil. Trans. R. Soc. Lond. B 1995 **349**, 353-364
doi: 10.1098/rstb.1995.0124

Heterogeneous morphology and tracer coupling patterns of retinal oligodendrocytes

EDITH C. G. M. HAMPSON AND STEPHEN R. ROBINSON

Vision, Touch and Hearing Research Centre, Department of Physiology and Pharmacology, The University of Queensland, Brisbane, QLD 4072, Australia

SUMMARY

The present study characterizes the morphology and tracer coupling patterns of oligodendrocytes in the myelinated band of the rabbit retina, as revealed by intracellular injection of biocytin or Lucifer yellow in an isolated superfused preparation. Based on the observed heterogeneity in morphology, we have grouped the presumptive oligodendrocytes into three categories termed 'parallel', 'stratified' and 'radial'. Most parallel oligodendrocytes were tracer coupled to nearby oligodendrocytes and astrocytes, whereas the stratified and radial oligodendrocytes rarely showed coupling. We conclude that the different categories of oligodendrocytes may be stages in a developmental series, with radial oligodendrocytes being premyelinating cells, parallel oligodendrocytes being mature myelinating cells and the stratified cells representing a transition between these categories.

1. INTRODUCTION

Oligodendrocytes are a class of neuroglia serving diverse functions within the central nervous system (CNS). In addition to enclosing segments of axons within insulating sheaths of myelin (Kruger & Maxwell 1966), oligodendrocytes appear to be involved in the regulation of extracellular K^+ (Barres *et al.* 1988, 1990; Sontheimer *et al.* 1989) and pH (Ghandour *et al.* 1979; Kumpulainen & Nyström 1981; Moscona 1983). Oligodendrocytes are commonly connected via gap junctions to astrocytes (Massa & Mugnaini 1982, 1985; Waxman & Black 1984) and less commonly to other oligodendrocytes (Dermietzel *et al.* 1978; Wollmann *et al.* 1981; Gonatas *et al.* 1982; cf. Massa & Mugnaini 1982, 1985; Massa *et al.* 1984). This coupling pattern may enable oligodendrocytes to contribute to syncytia that can serve as a 'spatial buffer' for K^+ regulation, as has been shown in astrocytes (Kuffler 1967; Brightman & Reese 1969; Orkland 1977; Gardner-Medwin 1983; Mobbs *et al.* 1988).

Most studies of the morphology and coupling properties of oligodendrocytes have used either cells grown *in vitro*, brain slices or preparations of isolated optic nerve. Like the optic nerve, the myelinated band of the rabbit retina contains both astrocytes and oligodendrocytes (Reichenbach *et al.* 1988; Scherer & Schnitzer 1991). As a model of white matter in the CNS, the myelinated band has the advantage that it can be readily isolated in an intact state, the tissue damage that is inevitable with brain slices thereby being avoided. Furthermore, the myelinated band is thin and flat, making it an ideal preparation for the investigation of oligodendrocytes *in situ* with intracellular injection techniques.

In a recent study (Robinson *et al.* 1993) oligodendrocytes in the isolated rabbit retina were injected with Lucifer yellow or the biotinylated tracer, biocytin. Both tracers revealed morphological heterogeneity among the injected cells. However, Lucifer yellow injected into oligodendrocytes rarely passed to neighbouring cells, while biocytin commonly passed to neighbours. Assessed in this way, some oligodendrocytes were coupled to large numbers of cells, while others were coupled to only a few or none at all. The aim of the present study was to investigate this heterogeneity in greater detail, paying particular attention to whether differences in the morphology of oligodendrocytes are matched by differences in their coupling patterns. Parts of this study have been reported in abstracts (Hampson *et al.* 1993, 1994).

2. MATERIALS AND METHODS

Nineteen pigmented rabbits of either sex (aged 6–16 weeks postnatal) were used. Procedures followed were in accord with the Australian code of practice for the care and use of animals for scientific purposes.

(*a*) *Isolated retinal preparations*

Adult pigmented rabbits of either sex (10–16 weeks postnatal) were given a lethal intravenous dose of sodium pentobarbitone (60 mg kg^{-1}). Pieces of living retina containing the myelinated band were isolated from sclera and flat-mounted onto black Millipore filters with the nerve fibre layer (NFL) uppermost. The flatmounts were immersed in Ames culture medium (Sigma) carboxygenated at room temperature (21 °C), pH 7.3 ± 0.2, and then incubated for 20 min in 100 ml of Ames medium (32 °C, pH 7.4 ± 0.2) containing 2 µg of Hoechst 38317, a fluorescent dye that stains the nuclei of neurons and most glia, excluding microglia (Vaney 1991; Robinson *et al.* 1993). Labelled astrocytes have ovoid nuclei (Choi & Kim 1985), whereas those of presumptive oligodendrocytes are circular or crescent-shaped.

(*b*) *Microinjection procedure*

This study was restricted to oligodendrocytes at the margin of the myelinated band, in a zone approximately 1 mm wide. Selected nuclei of presumed oligodendrocytes in this zone were visualized microscopically and impaled with a micropipette containing either 40 mg ml^{-1} Lucifer yellow CH dilithium salt (Sigma) in water, or a combination of 10 mg ml^{-1} Lucifer yellow and 30 mg ml^{-1} biocytin (Horikawa & Armstrong 1988; Sigma) in 0.1 M Tris buffer, pH 7.6. The 40 mg ml^{-1} Lucifer yellow was iontophoresed with a negative current of 0.5–1.0 nA for 30–60 s, whereas the 30 mg ml^{-1} was iontophoresed with a positive current of the same amplitude and duration. For further details see Vaney (1984, 1991) and Hampson *et al.* (1992).

(*c*) *Processing of retinal flatmounts*

The retinal flatmounts were immersion-fixed in 4% (by volume) paraformaldehyde and the biocytin was visualized by incubation with a streptavidin–biotinylated-HRP complex (Amersham) with diaminobenzidine (Sigma) as the chromagen (Vaney 1991; Hampson *et al.* 1992). The diaminobenzidine reaction product was photochromically intensified in the presence of 0.2 mg ml^{-1} nitro blue tetrazolium in 0.1 M Tris buffer (pH 8.2; Vaney 1992).

(*d*) *Morphological analysis of biocytin-filled cells*

Fifty-eight presumed oligodendrocytes from the retinae of seven rabbits were completely filled with biocytin. These cells were viewed with a Zeiss Axioplan with DIC optics with the use of a ×100 objective (final magnification ×1250). Drawings of their morphology were prepared by using a drawing tube and the following features were measured.

1. The maximum length (i.e. the longest axis of the cell), width (i.e. orthogonal to the longest axis) and the depth of the field occupied by the processes of each cell. Depth was calculated from the scale on the fine focus of the microscope.
2. The area of the field of labelled processes.
3. The length of individual processes, or parts thereof, that extend parallel to the axons in the NFL (i.e. potential myelinating processes).
4. The area of the profile of each soma (i.e. product of maximum length and width).

It was not always possible to measure every feature, because some cells were partly obscured by biocytin in overlying Müller cell endfeet. This inadvertent labelling resulted from the fact that the micropipette had to pass through the endfeet of Müller cells composing the inner limiting membrane (Holländer *et al.* 1991).

(*e*) *Analysis of tracer coupling*

In addition to the 58 presumed oligodendrocytes that were drawn, a further 15 oligodendrocytes were included in the analysis of tracer coupling. For these analyses we counted: (1) the number of injected cells that showed tracer coupling, (2) the number of cells that were coupled to each injected cell and (3) the area of retina encompassed by the field of cells coupled to each injected cell.

(*f*) *Immunocytochemical labelling for GFAP*

Retinas from adult rabbits aged 10–12 weeks ($n = 3$) and a juvenile rabbit aged 6 weeks were immunolabelled with the specific astrocyte marker, glial fibrillary acidic protein (GFAP; Schnitzer 1985). All retinas were processed by immunofluorescence methods and examined to determine whether cells injected with Lucifer yellow were GFAP$^+$. Retinas were immersion-fixed in 4% paraformaldehyde in 0.1 M phosphate buffer (pH 7.2) for 1 h, washed in phosphate buffered saline (PBS, pH 7.3), and then incubated overnight in PBS containing 1 mg ml^{-1} bovine serum albumin (BSA) and 0.5% (by volume) Triton X-100. Thereafter, the tissue was washed in PBS and incubated for 10 days with mouse GFAP antiserum (Boehringer) diluted 1:30 in PBS containing 10 mg ml^{-1} BSA, 0.5% Triton X-100 and 0.5 mg ml^{-1} sodium azide. The tissue was then washed in PBS and incubated for 4 h with sheep anti-mouse secondary antibody conjugated to Texas Red (Amersham). The antibody was diluted 1:50 in PBS containing 10 mg ml^{-1} BSA, 0.5% (by volume) Triton X-100 and 0.5 mg ml^{-1} sodium azide. The tissue was finally washed and mounted in glycerol:PBS (1:1).

(*g*) *Immunocytochemical labelling with Rip antibody*

Retinas from seven adult rabbits were immunolabelled with the mouse monoclonal antibody 'Rip', a highly specific oligodendrocyte marker (Friedman *et al.* 1989). Retinas were immersion-fixed for 6 h, washed overnight in PBS containing 0.5% (by volume) Triton X-100 and then incubated for 1 h in PBS containing 1 mg ml^{-1} BSA and 0.5% (by volume) Triton X-100. The tissue was then incubated with Rip antibody (supernatant, undiluted containing 2% Triton X-100), at dilutions of 1:1, 1:5, 1:10 or 1:20 in PBS with 1 mg ml^{-1} BSA, 0.5% (by volume) Triton X-100 and 0.5 mg ml^{-1} sodium azide. Control sections were incubated as described above, but the Rip antibody was replaced with non-immune mouse serum. After incubation for 2–7 days, the tissue was washed in PBS and incubated overnight with biotinylated sheep anti-mouse immunoglobulin (Amersham) at a dilution of 1:300 in PBS containing 1 mg ml^{-1} BSA. Thereafter, the tissue was washed in PBS and incubated for 6 h with strepavidin–HRP diluted 1:300 in PBS containing 1 mg ml^{-1} BSA. The tissue was then reacted with diaminobenzidine and the labelling intensified with nitro blue tetrazolium (Vaney 1992), as described above.

The somata of 177 oligodendrocytes labelled with Rip from three retinal pieces were drawn and their maximum length, width and area were measured.

(*h*) *Confocal microscopy*

Confocal microscopy was done with a Bio-Rad MRC-600 confocal laser scanning microscope mounted on a Zeiss Axioskop. Tissue was viewed through a ×40 oil immersion objective. Lucifer yellow fluorescence was observed by exciting the tissue with the 488 nm line of an argon–krypton laser and using the dual-excitation K1/K2 filter blocks to gather the green emitting signal. Images were collected with use of a z-step of 1 μm. Subsequently, GFAP immunofluorescence was observed by exciting the tissue with the 568 nm line and using the dual excitation K1/K2 filter blocks to gather the red emitting signal. Images were collected over the same region and depth interval as used for Lucifer yellow, but a z-step of 2 μm was used. These individual z-series were projected, and merged by using Adobe Photoshop 2.5.1. to provide a composite image of the injected cell and its associated GFAP immunoreactivity.

PHILOSOPHICAL TRANSACTIONS OF THE ROYAL SOCIETY B BIOLOGICAL SCIENCES

3. RESULTS

Considerable heterogeneity was observed among the presumptive oligodendrocytes injected in this study. Our identification of oligodendrocytes was based on the following criteria. (1) The cells had circular or crescent-shaped nuclei, rather than ovoid ones, which are characteristic of astrocytes (Choi & Kim 1985). (2) The filled cells did not resemble any morphological class of astrocyte already described in the rabbit retina (Schnitzer & Karschin 1986; Robinson & Dreher 1989; Triviño *et al.* 1992). Furthermore, as will be shown in these results, (3) the presumptive oligodendrocytes injected with Lucifer yellow were $GFAP^{-}$, whereas presumptive astrocytes were $GFAP^{+}$. (4) The injected oligodendrocytes resembled those that were

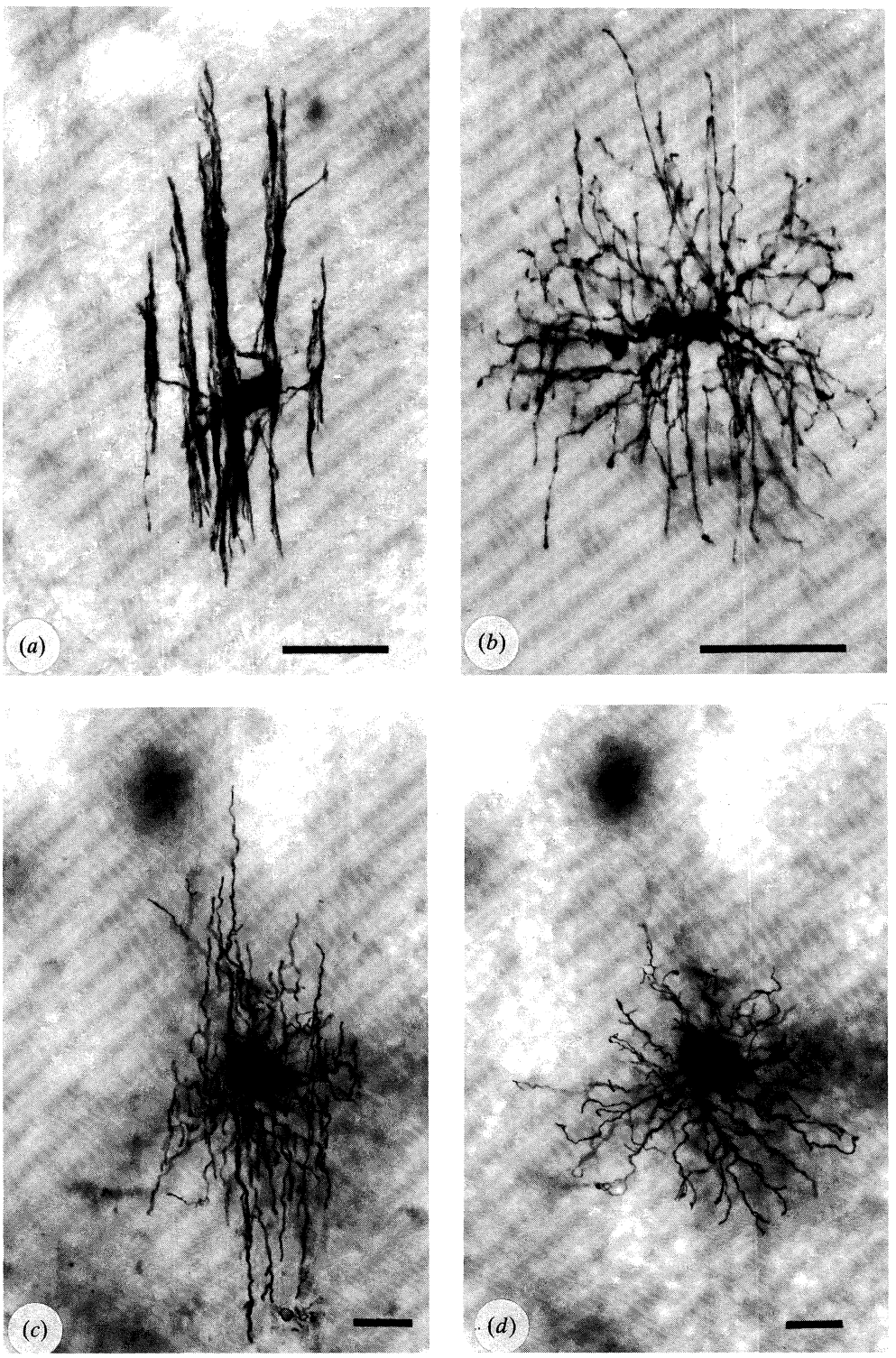

Figure 1. Photomicrographs of oligodendrocytes injected with biocytin. (*a*) A parallel oligodendrocyte with processes in the NFL. (*b*) A radial oligodendrocyte with processes radiating in all directions within the NFL. (*c*, *d*) A stratified oligodendrocyte with parallel processes within the NFL (*c*), and deeper radial processes within the IPL (*d*). Scale bars 30 μm.

PHILOSOPHICAL TRANSACTIONS OF THE ROYAL SOCIETY B BIOLOGICAL SCIENCES

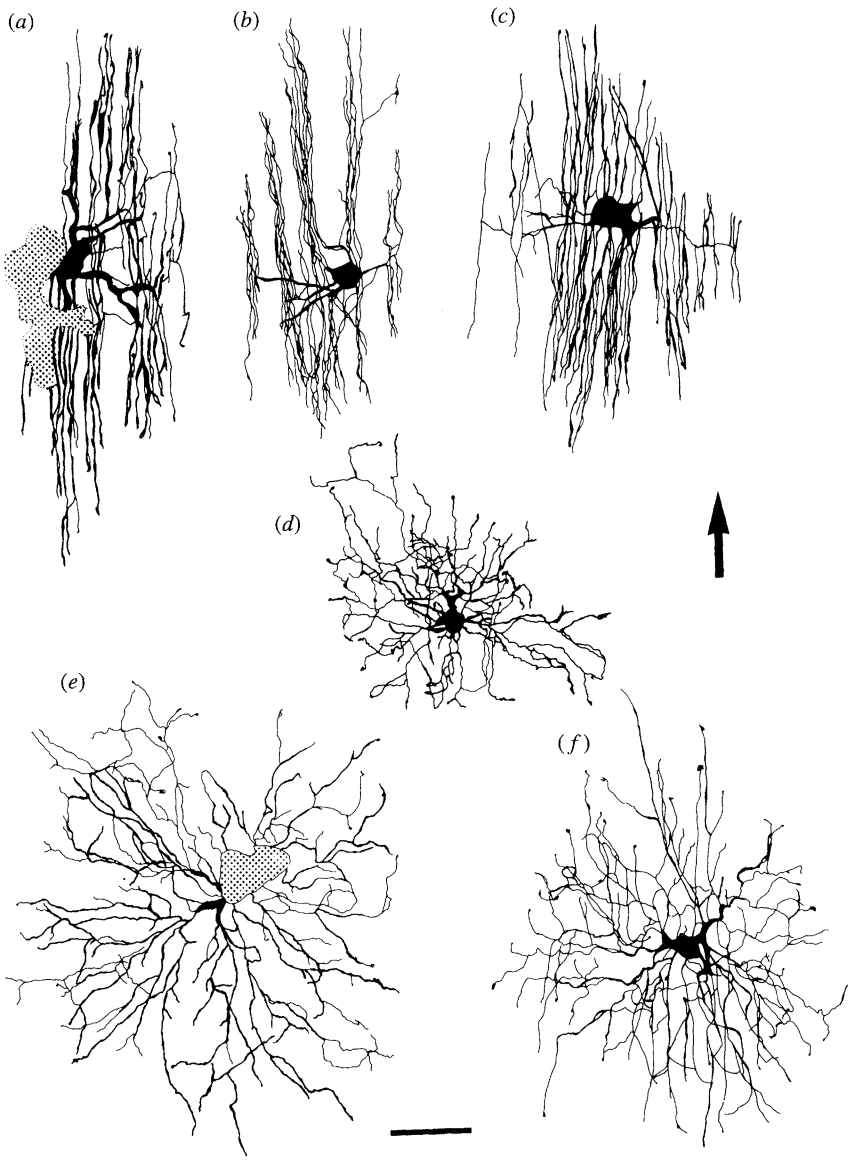

Figure 2. Drawings of parallel and radial oligodendrocytes illustrating the variation in their morphology. (*a–c*) Parallel oligodendrocytes with processes within the NFL. (*d–f*) Radial oligodendrocytes with processes radiating in all directions within the NFL. Note the terminal varicosities on these processes. The arrow is parallel to the axons in NFL and the arrowhead points towards the optic nerve head. The stippled areas in (*a*) and (*e*) represent adjacent Müller cells which were filled with biocytin during the removal of the micropipette after injection. Scale bar 30 μm.

immunoreactive for the highly specific oligodendrocyte marker, Rip (Friedman *et al.* 1989). (5) The injected oligodendrocytes had identical soma dimensions to Rip^+ cells.

From a comparison of their morphology, we grouped the injected oligodendrocytes into three categories termed 'parallel', 'stratified' and 'radial'. These morphological differences were matched by differences in their coupling patterns. Cells from all three categories were common throughout the zone of retina investigated.

(*a*) *Morphology and tracer coupling patterns of oligodendrocytes filled with biocytin*

Parallel oligodendrocytes have thin primary processes that radiate from the soma and give rise to thicker secondary processes. These thicker processes exhibit a strong tendency to fasciculate with each other as they extend parallel to the axons in the NFL (figures 1*a*, 2*a–c*, 5*a*). When compared with cells in the other two categories, parallel oligodendrocytes have a relatively large soma and their processes occupy a shallow rectangular field (table 1). They also have a greater number and length of myelinating processes in the NFL.

Parallel oligodendrocytes represented 45% ($n = 33$) of the 73 cells injected with biocytin; 52% ($n = 17$) of these 33 cells showed tracer coupling to 64 ± 46 presumed oligodendrocytes and astrocytes (figure 3, table 2). Oligodendrocytes coupled to the injected cells were not labelled well enough to be grouped into the three categories. The mean area of retina encompassed by the field of cells coupled to each injected cell was 3.6 ± 5.6 mm² (table 2).

Radial oligodendrocytes have thin processes that radiate in all directions. These processes show only a slight tendency to follow axons in the NFL. Compared with the processes of parallel oligodendrocytes, those of

Table 1. *Morphometry of oligodendrocyte processes and somata*

feature	parallel	stratified	radial
mean max. length of field/μm	171.5±45.6	187.9±38.6	153.0±34.1
mean max. width of field/μm	74.6±22.2	104.9±29.9	102.2±35.1
mean max. depth of field/μm	14.6±4.2	30.8±14.0	14.8±11.2
mean field area/μm²	8332±1072	11 133±3624	8746±4323
mean number of myelinating processes[a]	56±12	NFL: 33±13 GCL: 46±5 IPL: 22±16	23±5
total length of myelinating processes/μm	2767±664	NFL: 987±441 GCL: 1756±114 IPL: 488±347	528±266
mean area of soma/μm²	104.4±41.2	105.4±46.6	66.5±31.1

[a] 'Myelinating' processes are processes, or segments thereof, that extend parallel to the axons in the NFL.

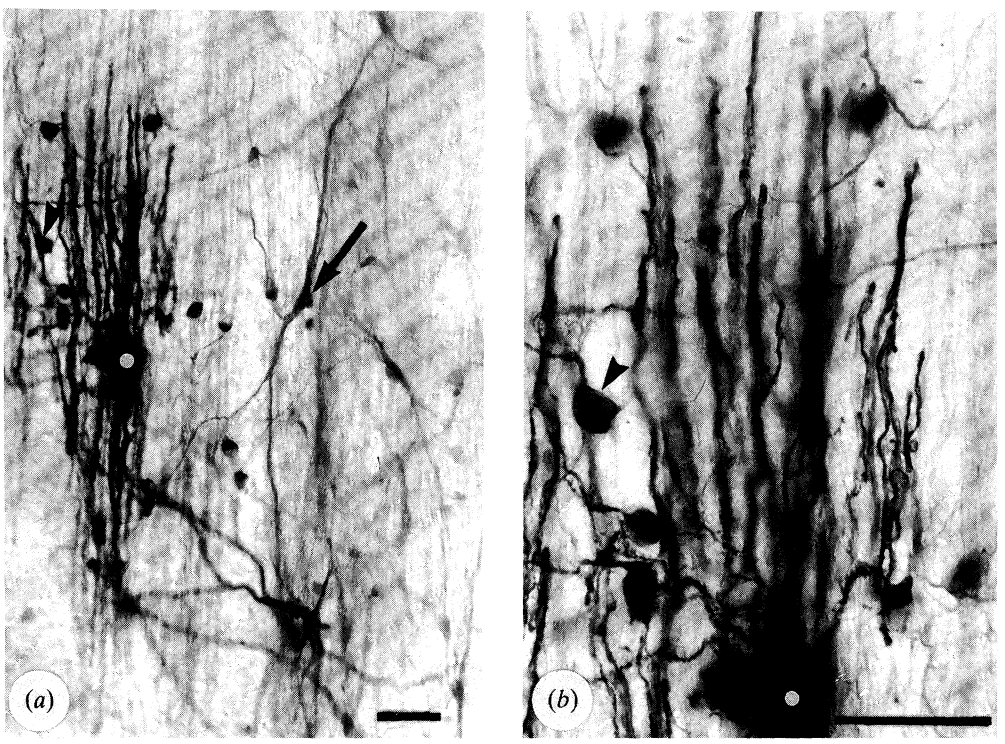

Figure 3. Photomicrographs taken at low magnification (*a*) and high magnification (*b*) illustrating the extent of tracer coupling between an injected parallel oligodendrocyte (bullseye) and neighbouring oligodendrocytes (arrowhead) and astrocytes (arrow) within the NFL. Scale bars 30 μm.

Table 2. *Comparison of the extent of tracer coupling in three categories of oligodendrocyte*

category of oligodendrocyte	no. of injected cells	no. of injected cells that were tracer coupled	mean no. of coupled cells per tracer coupled cell (x±s.d.)	mean area covered by tracer coupled cells/mm²
parallel	33	17 (52%)	64±46	3.6±5.6
stratified	30	4 (13%)	45±30	4.2±3.7
radial	10	1 (10%)	5.0	0.06

radial cells are thinner, branch more profusely and follow a more tortuous course through the neuropil. These processes consistently terminate in varicosities (figures 1*b*, 2*d–f*, 5*b*, *c*). The field occupied by the processes of these cells is shorter and wider than that of parallel oligodendrocytes, but both have a similar field area and depth (table 1). Radial cells have few processes that extend parallel to axons in the NFL. Those that do so extend for only a short distance, so that radial oligodendrocytes have far fewer 'myelinating' processes than other oligodendrocytes. In summary, the radial cells have the smallest somata and their processes occupy a shallow circular field.

Radial oligodendrocytes represented 14% (n = 10) of the 73 cells injected with biocytin; only one of these ten cells showed tracer coupling. This cell was coupled

PHILOSOPHICAL TRANSACTIONS OF THE ROYAL SOCIETY B BIOLOGICAL SCIENCES

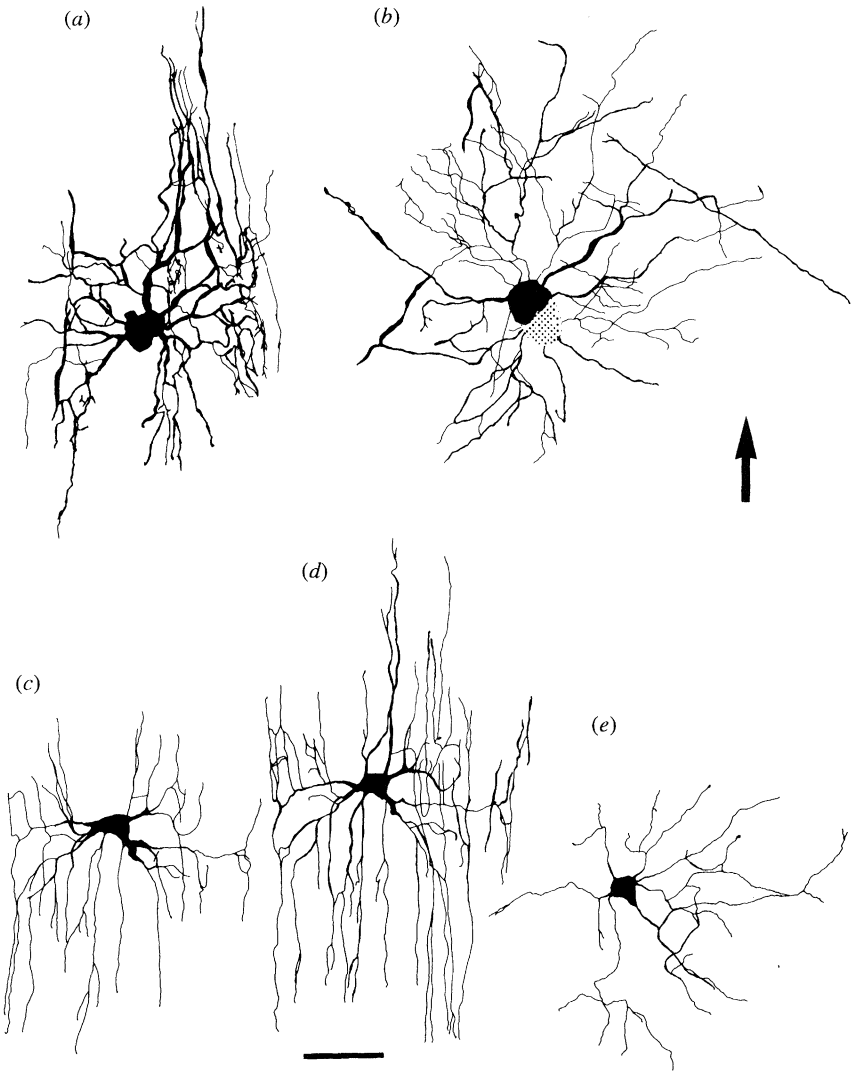

Figure 4. Drawings of stratified oligodendrocytes illustrating variation in their morphology. (*a*, *b*) An oligodendrocyte with processes extending parallel to the axons in the NFL (*a*) and a second plexus radiating in all directions in the GCL (*b*). (*c–e*) An oligodendrocyte with parallel processes in a superficial stratum of the NFL (*c*) and a deeper stratum of the NFL (*d*), as well as radial processes in the IPL (*e*). The stippled area in (*b*) represents an adjacent Müller cell which was filled with biocytin during the removal of the micropipette after injection. Scale bar 30 μm.

to five other presumptive oligodendrocytes and the total coupled field encompassed an area of 0.06 mm² (table 2).

Stratified oligodendrocytes have two plexuses of processes. One is located in the NFL and ganglion cell layer (GCL) and resembles that of 'parallel' oligodendrocytes, except that the processes of the stratified oligodendrocytes show less tendency to form fascicles with each other. The second deeper plexus terminates in the GCL or inner plexiform layer (IPL) and resembles that of 'radial' oligodendrocytes, except that the processes of stratified oligodendrocytes are restricted to one or two narrow strata (figures 1*c*, *d*, 4*a–e*, 5*e*, *f*). The field occupied by the processes of stratified oligodendrocytes is longer than that of radial cells, wider than that of parallel cells and occupies a larger retinal area than parallel cells (table 1). In addition, their processes extend through a greater depth than those of either parallel or radial cells. Moreover, the somata of stratified oligodendrocytes are larger than those of radial cells (compare figures 4*a–e* with 2*d–f*). When the lengths of myelinating processes in the NFL and GCL are measured, the combined values obtained for the stratified oligodendrocytes closely resemble those for parallel oligodendrocytes. Similarly, the lengths of stratified oligodendrocyte processes in the IPL resemble those of radial oligodendrocytes (table 1). In summary, stratified oligodendrocytes have large somata and their processes occupy a deep rectangular field.

Stratified oligodendrocytes represented 41% ($n = 30$) of the 73 cells injected with biocytin; only four of these 30 cells showed tracer coupling, labelling 45 ± 30 oligodendrocytes and astrocytes. The mean area of retina encompassed by the field of coupled cells was 4.2 ± 3.7 mm² (table 2).

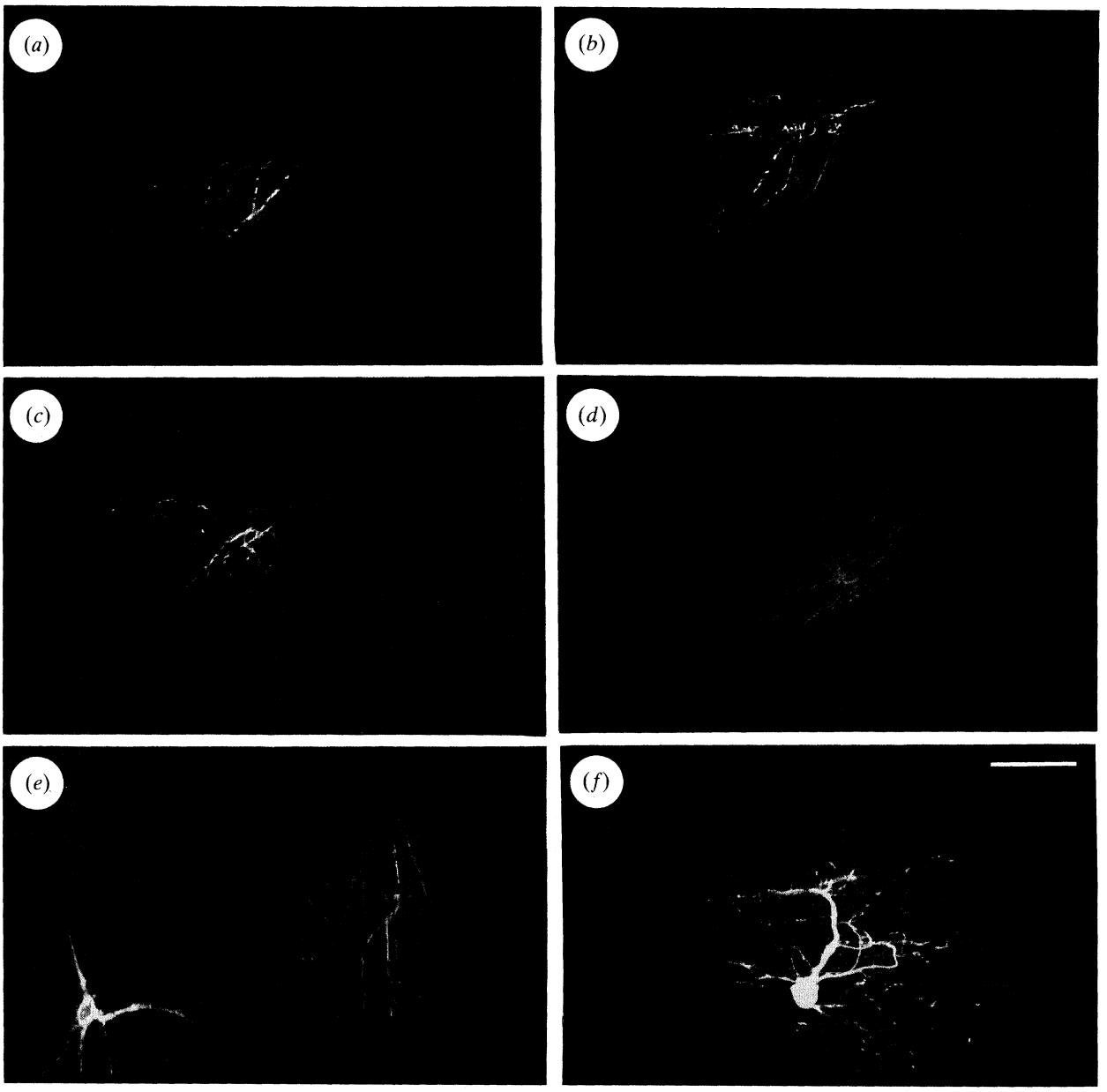

Figure 5. Pseudocolour composite confocal images of oligodendrocytes and astrocytes obtained from a 6 week old rabbit. (*a–e*) Oligodendrocytes injected with Lucifer yellow (green) show morphological heterogeneity, but are not GFAP$^+$, unlike adjacent astrocytes (red). (*a*) A parallel oligodendrocyte with processes in the NFL. (*b*, *c*) Radial oligodendrocytes with processes in the NFL. (*d*) An oligodendrocyte with radiating and parallel processes in the same layer. (*e*) A periaxonal astrocyte injected with Lucifer yellow is also GFAP$^+$ (yellow). A nearby stratified oligodendrocyte (green) is GFAP$^-$. (*f*) Image of the oligodendrocyte injected with Lucifer yellow in (*e*). The cell has been magnified and rotated counterclockwise by 90°. GFAP immunoreactivity is not shown. The superficial, parallel processes of the cell are depicted in green, the intermediate processes are coloured yellow and the deep radial processes are red. Scale bar 50 μm (*a–e*) and 30 μm (*f*).

(*b*) *GFAP immunoreactivity and morphology of oligodendrocytes injected with Lucifer yellow*

Oligodendrocytes injected with Lucifer yellow (n = 54) had a very similar morphology to those injected with biocytin. These oligodendrocytes could also be categorized as parallel, stratified or radial cells. Representatives of all three categories were found from the earliest age examined (6 weeks postnatal; figure 5) and they composed similar proportions of the overall population at each age, although radial cells tended to be more frequently encountered in the 6 week retina.

None of the oligodendrocytes injected with Lucifer yellow were GFAP$^+$ (figure 5*a–e*). By contrast, strong GFAP immunoreactivity was found in perivascular and periaxonal astrocytes that had been injected with Lucifer yellow (figure 5*e*). The absence of GFAP immunoreactivity from presumptive oligodendrocytes is not due to a failure of the antibody to penetrate the myelinated band, since GFAP$^+$ astrocytes were often found at the same depth and directly adjacent to oligodendrocytes injected with Lucifer yellow (figures 5*a–e*).

PHILOSOPHICAL TRANSACTIONS OF THE ROYAL SOCIETY B BIOLOGICAL SCIENCES

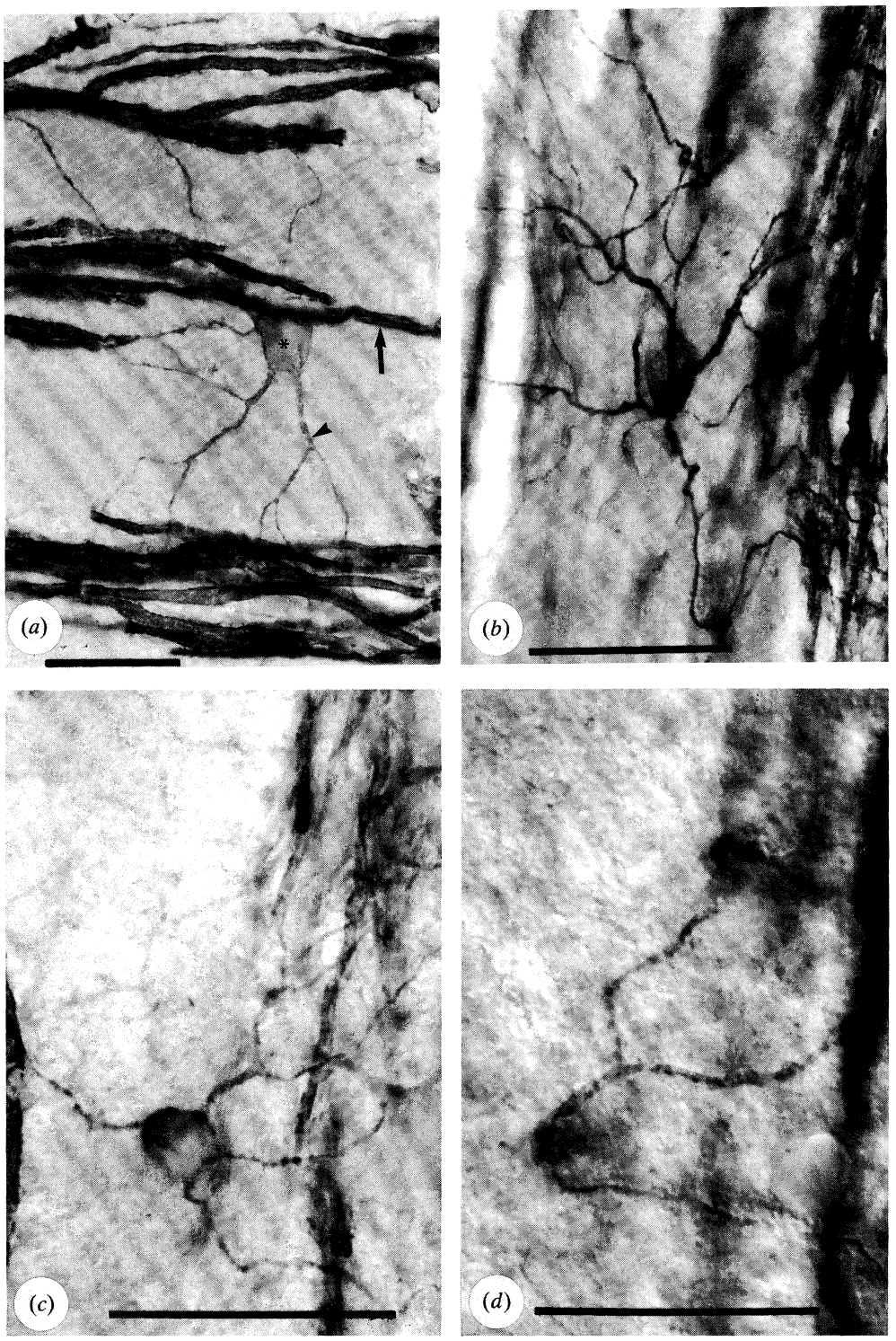

Figure 6. Photomicrographs of Rip immunoreactivity in retinal oligodendrocytes. (*a*) A presumptive parallel oligodendrocyte (asterisk) with fine radial branches (arrowhead) that connect with thicker parallel processes (myelin sheaths; arrow) that run parallel to the axons in the NFL. (*b*) A presumptive radial oligodendrocyte with fine recurving processes in the NFL. (*c*, *d*) A presumptive stratified oligodendrocyte with processes ramifying in both the NFL (*c*) and the IPL (*d*). Scale bars 30 μm.

(*c*) *Morphology of Rip-immunolabelled oligodendrocytes*

The Rip antibody lightly labelled the somata and thicker processes of many oligodendrocytes and intensely labelled their myelin sheaths (which are not evident in cells filled with Lucifer yellow or biocytin). The failure of the antibody to label many of the finer processes prevented morphometric analysis of their branching patterns and resulted in a sparser appearance in micrographs compared with injected cells (figure 6). No Rip-immunolabelled processes were seen in any retinal layer beyond the limits of the myelinated band. Most labelled oligodendrocytes had processes

that extended within a narrow stratum of the NFL. Their primary branches radiated from the soma and gave rise to secondary and tertiary processes that aligned parallel to the axons in the NFL and appeared to contribute to the myelin sheaths of these axons (figure 6*a*). A few oligodendrocytes had processes that ramified within two strata. The processes in the superficial stratum resembled those of parallel oligodendrocytes, except that they were fewer in number (figure 6*c*). Within the deeper stratum, a few processes radiated from the soma (figure 6*d*). These processes were thicker than those in the superficial layer, had a sparse branching pattern and followed a fairly direct course through the neuropil. Rip-immunolabelled processes were common within this deeper stratum but, in most cases, they could not be traced to their cell of origin. Very occasionally, oligodendrocytes had radiating primary processes that followed a tortuous recurving course and did not align themselves with the axons in the NFL (figure 6*b*).

Measurements of the somata of Rip^+ cells revealed close similarities with the population of biocytin-injected cells. Thus, the Rip^+ cells had maximum soma lengths ranging from 7 to 20 μm, while those of injected cells ranged between 6 and 19 μm. Similarly, their maximum widths ranged from 6 to 12 μm and from 4 to 15 μm, respectively. The total area of their somata ranged from 40 to 200 μm^2 in Rip^+ cells and from 21 to 238 μm^2 in cells injected with biocytin. The mean area of somata in the two groups was 98 μm^2 (s.d. 32 μm^2) and 98 μm^2 (s.d. 44 μm^2), respectively. There was no significant difference in the area of somata between the two groups (unpaired *t*-test; $p < 0.980$).

Attempts to demonstrate convincingly Rip immunoreactivity in presumptive oligodendrocytes that had been injected with Lucifer yellow were unsuccessful. This was due to the fact that, in our hands, the Rip antibody produced faint labelling of somata and most processes, especially when processed by the immunofluorescence methods that are necessary for demonstrating double labelling.

4. DISCUSSION

We have examined the morphology and tracer coupling patterns of oligodendrocytes in the myelinated band of the rabbit retina following intracellular injection of Lucifer yellow or biocytin. This study provides the first detailed description of retinal oligodendrocytes and is the most comprehensive morphometric description of oligodendrocytes from anywhere in the CNS.

The myelinating oligodendrocytes described here are similar to the myelinating oligodendrocytes in other regions of the nervous system. For example, mature oligodendrocytes in the rat optic nerve have 15–20 myelinating processes within a field 150–250 μm in length and 30–60 μm in width (Butt & Ransom 1989, 1993; Ransom *et al.* 1991; Butt *et al.* 1994). Parallel oligodendrocytes in the myelinated band of the rabbit retina have an average of 56 myelinating processes that extend over a mean field length of 171 μm and mean field width of 75 μm. Oligodendrocytes of a similar appearance and size have also been illustrated in micrographs from rabbit retina stained with sulphorhodamine 101 (Ehinger *et al.* 1994) and from Rip-immunolabelled sections of rat hippocampus (Berger & Frotscher 1994) and hamster brain (Jhaveri *et al.* 1992).

In addition to providing useful baseline data, the present study revealed some new features, which are discussed below.

(*a*) *Heterogeneity among retinal oligodendrocytes*

On the basis of their morphology, we grouped the injected oligodendrocytes into three categories. *Parallel* oligodendrocytes resemble 'classical' myelinating oligodendrocytes and have numerous processes aligned parallel to the axons in the NFL. They occupy a shallow rectangular field and are often extensively coupled. All the oligodendrocytes that showed tracer coupling had myelinating processes, which suggests that the cell coupling may be involved with servicing myelin sheaths. Gap junctions, for example, may connect oligodendrocytes into syncytia, making them better able to serve as a spatial buffer for local fluctuations in extracellular K^+ (Barres *et al.* 1988).

Stratified oligodendrocytes have a superficial field of processes in the NFL and GCL that resembles those of parallel oligodendrocytes, and a deeper radial field of processes that ramifies within the IPL. Stratified oligodendrocytes occasionally showed tracer coupling. As far as we are aware, oligodendrocyte processes have not been reported previously in the IPL. The Rip immunolabelling indicates that some of the oligodendrocyte processes in this layer form myelinating sheaths. Since the density of these segments was comparatively low, they could only be associated with a small proportion of the axons or dendrites in that layer. The element that they are most likely to be associated with is the axons of displaced ganglion cells, since these often course for some distance in the IPL before entering the NFL (unpublished observations), but they may also be associated with the long range processes of 'axon bearing' amacrine cells.

Radial oligodendrocytes rarely showed tracer coupling and closely resembled the deep processes of stratified cells. Oligodendrocytes with a radial morphology were first described in the white and grey matter of the CNS by Del Río-Hortega (1928). These 'type I' oligodendrocytes are small with fine radial processes which do not appear to be connected to myelin (Bunge 1968). More recently, others have reported similar oligodendrocytes in the CNS of immature cats (Rámon-Moliner 1958) and adult rats (Friedman *et al.* 1989). Since their morphology precludes a role in myelination, radial oligodendrocytes may be premyelinating cells (see conclusions).

(*b*) *Cell coupling*

Investigations of dye coupling in oligodendrocytes injected with Lucifer yellow (457 Da) have concluded that these cells are either weakly coupled to a few

PHILOSOPHICAL TRANSACTIONS OF THE ROYAL SOCIETY B BIOLOGICAL SCIENCES

adjacent cells or not coupled at all (see, for example: Butt & Ransom 1989, 1993; Von Blankenfeld *et al.* 1993). Electrophysiological studies have reached similar conclusions (see, for example: Ransom & Kettenmann 1990; Von Blankenfeld *et al.* 1993). By contrast in the present study 30% of the oligodendrocytes injected with biocytin showed tracer coupling to other cells. Moreover, the biocytin coupled oligodendrocytes were coupled to many neighbouring cells (e.g. a mean of 64 cells for parallel oligodendrocytes) and, contrary to previous reports (see, for example, Butt & Ransom 1989), oligodendrocytes showed tracer coupling to both oligodendrocytes and astrocytes (e.g. figure 3).

It is now widely appreciated that injections with biocytin demonstrate more extensive coupling than is evident from injections with dyes of higher molecular mass (Vaney 1991). Indeed, oligodendrocytes injected with Lucifer yellow in this and a previous study (Robinson *et al.* 1993) showed little, if any, dye coupling (figure 5). The tracer coupling revealed by biocytin injections show that some oligodendrocytes are much more extensively coupled than was previously assumed. These findings increase the likelihood that gap junctions serve as an important avenue of intercellular communication between oligodendrocytes. It should be noted, however, that 70% of the oligodendrocytes injected with biocytin failed to exhibit any tracer coupling. We do not yet know whether these cells are unidirectionally coupled (Robinson *et al.* 1993) or show tracer coupling under other physiological conditions.

Studies in rat optic nerve have reported that dye coupling between oligodendrocytes occurs via contacts between adjacent cell bodies (Butt & Ransom 1993). In our material, coupled cells were found both within and beyond the field occupied by the processes of injected oligodendrocytes. Thus, our findings indicate that coupling is more likely to be mediated by gap junctions between the processes of adjacent oligodendrocytes.

(*c*) *Conclusions*

Morphological heterogeneity has been recognized in other glial populations in the CNS, particularly among retinal astrocytes. There is uncertainty regarding the significance of this variability. Some authors regard the variation as being indicative of several distinct classes of cell (see, for example: Schnitzer & Karschin 1986; Miller *et al.* 1989; Robinson & Dreher 1989; Triviño *et al.* 1992), while others recognize a single cell class with a morphology that varies in response to microenvironmental factors or maturity (see, for example: Stone & Dreher 1987; Suárez & Raff 1989; Chan-Ling & Stone 1991).

Is the heterogeneity described in this study indicative of three distinct morphological classes of oligodendrocyte, or do the cells belong to a single class that shows a considerable degree of variability? At present, the weight of evidence favours the latter. Studies of the developing CNS have shown that immature premyelinating oligodendrocytes have a radial morphology. As they mature, these cells extend new processes that ensheath axons and coincident with this differentiation the cells lose or retract their radial field (see, for example: Rámon-Moliner 1958; Jhaveri *et al.* 1992; Butt & Ransom 1993). The sequence of maturation among oligodendrocytes is also accompanied by an increase in the incidence of tracer coupling (Von Blankenfeld *et al.* 1993). Thus, the radial oligodendrocytes observed in this study may be premyelinating cells, while stratified cells may be in the process of differentiating into mature myelinating (parallel) oligodendrocytes.

It is possible that radial and stratified oligodendrocytes are cells in arrested stages of differentiation and represent a pool of cells that can be used to replace damaged oligodendrocytes as the retina ages. Indeed, a population of premyelinating, multipolar oligodendrocytes has recently been described in the myelinated band of the adult rabbit retina (Chan-Ling & Morcos 1995). These oligodendrocytes, which are $O4^+/Gal\text{-}C^-/MBP^-$, have a morphology that closely resembles the radial oligodendrocytes described in the present study (Y. Morcos, personal communication).

One would expect that dormant premyelinating cells should have a simple undifferentiated morphology, since in this form they would require less energy and space. The fact that the radial oligodendrocytes have a highly complex, differentiated morphology raises the possibility that these cells are specialized to perform some other function in the interim.

We thank D. Noone, D. Crook and C. Nelson for invaluable assistance. D. Pow, R. Tweedale and D. I. Vaney provided constructive comments on the manuscript. C. L. Macqueen provided technical assistance with the confocal microscopy. The mouse monoclonal antibody Rip was a generous gift from B. Friedman (Regeneron Pharmaceuticals, Tarrytown, New York), M. Pender and K. Nguyen. This work was supported by a National Health and Medical Research Council project grant to D. I. Vaney and by grants to S. R. Robinson from the Australian Research Council.

REFERENCES

Barres, B. A., Chun, L. L. Y. & Corey, D. P. 1988 Ion channel expression by white matter glia: I. Type 2 astrocytes and oligodendrocytes. *Glia* **1**, 10–30.

Barres, B. A., Chun, L. L. Y. & Corey, D. P. 1990 Ion channels in vertebrate glia. *A. Rev. Neurosci.* **13**, 441–474.

Berger, T. & Frotscher, M. 1994 Distribution and morphological characteristics of oligodendrocytes in the rat hippocampus *in situ* and *in vitro*: an immunocytochemical study with the monoclonal Rip antibody. *J. Neurocytol.* **23**, 61–74.

Brightman, M. W. & Reese, T. S. 1969 Junctions between intimately apposed cell membranes in the vertebrate brain. *J. Cell Biol.* **40**, 648–677.

Bunge, R. P. 1968 Glial cells and the central myelin sheath. *Physiol. Rev.* **48**, 197–251.

Butt, A. M. & Ransom, B. R. 1989 Visualization of oligodendrocytes and astrocytes in the intact rat optic nerve by intracellular injection of Lucifer yellow and horseradish peroxidase. *Glia* **2**, 470–475.

Butt, A. M. & Ransom, B. R. 1993 Morphology of

PHILOSOPHICAL TRANSACTIONS OF THE ROYAL SOCIETY B BIOLOGICAL SCIENCES

astrocytes and oligodendrocytes during development in the intact rat optic nerve. *J. comp. Neurol.* **338**, 141–158.

Butt, A. M., Colquhoun, K. & Berry, M. 1994 Confocal imaging of glial cells in the intact rat optic nerve. *Glia* **10**, 315–322.

Chan-Ling, T. & Stone, J. 1991 Factors determining the morphology and distribution of astrocytes in the cat retina: a 'contact-spacing' model of astrocyte interaction. *J. comp. Neurol.* **303**, 387–399.

Chan-Ling, T. & Morcos, Y. 1995 *In vivo* evidence of oligodendrocyte precursors in the myelinated streak of the adult rabbit retina. *Proc. Aust. Neurosci. Soc.* **6**, 145.

Choi, B. H. & Kim, R. C. 1985 Expression of glial fibrillary acidic protein by immature oligodendroglia and its implications. *J Neuroimmunol.* **8**, 215–235.

Del Río-Hortega, P. 1928 Tercera aportación al conocimiento morfológico e interpretatción funcional de la oligodendroglía. *Mem. Real. Soc. Espan. Hist. nat.* **14**, 5–122.

Dermietzel, R., Schünke, D. & Leibstein, A. 1978 The oligodendrocytic junctional complex. *Cell Tiss. Res.* **193**, 61–72.

Ehinger, B., Zucker, C. L., Bruun, A. & Adolph, A. 1994 *In vivo* staining of oligodendroglia in the rabbit retina. *Glia* **10**, 40–48.

Friedman, B., Hockfield, S., Black, J. A., Woodruff, K. A. & Waxman, S. G. 1989 *In situ* demonstration of mature oligodendrocytes and their processes: an immunocytochemical study with a new monoclonal antibody, Rip. *Glia* **2**, 380–390.

Gardner-Medwin, A. R. 1983 Analysis of potassium dynamics in mammalian brain tissue. *J. Physiol., Lond.* **335**, 393–426.

Ghandour, M. S., Langley, O. K., Vincendon, G. & Gombos, G. 1979 Double labeling immunohistochemical technique provides evidence of the specificity of glial cell markers. *J. Histochem. Cytochem.* **27**, 1634–1637.

Gonatas, N. K., Hirayama, M., Stieber, A. & Silberberg, D. H. 1982 The ultrastructure of isolated rat oligodendrogial cell cultures. *J. Neurocytol.* **11**, 997–1008.

Hampson, E. C. G. M., Robinson, S. R. & Noone, D. 1994 Tracer injection reveals the morphology of retinal oligodendrocytes. *Proc. Aust. Neurosci. Soc.* **5**, 120.

Hampson, E. C. G. M., Robinson, S. R. & Vaney, D. I. 1993 Tracer-coupling reveals three classes of oligodendrocyte in rabbit retina. *Soc. Neurosci. Abstr.* **19**, 1118.

Hampson, E. C. G. M., Vaney, D. I. & Weiler, R. 1992 Dopaminergic modulation of gap junction permeability between amacrine cells in mammalian retina. *J. Neurosci.* **12**, 4911–4922.

Holländer, H., Makarov, F., Dreher, Z., van Driel, D., Chan-Ling, T. & Stone, J. 1991 Structure of the macroglia of the retina: the sharing and division of labour between astrocytes and Müller cells. *J. comp. Neurol.* **313**, 587–603.

Horikawa, K. & Armstrong, W. E. 1988 A versatile means of intracellular labeling: injection of biocytin and its detection with avidin conjugates. *J. Neurosci. Meth.* **25**, 1–11.

Jhaveri, S., Erzurumlu, R. S., Friedman, B. & Schneider, G. E. 1992 Oligodendrocytes and myelin formation along the optic tract of the developing hamster: an immunohistochemical study using the Rip antibody. *Glia* **6**, 138–148.

Kruger, L. & Maxwell, D. 1966 Electron microscopy of oligodendrocytes in normal rat cerebrum. *Am. J. Anat.* **118**, 411–435.

Kuffler, S. W. 1967 The Ferrier Lecture. Neuroglial cells: physiological properties and a potassium mediated effect of neuronal activity on the glial membrane potential. *Proc. R. Soc. Lond.* B **168**, 1–21.

Kumpulainen, T. & Nyström, S. H. M. 1981 Immunohistochemical localization of carbonic isoenzyme C in human brain. *Brain Res.* **220**, 220–225.

Massa, P. T. & Mugnaini, E. 1982 Cell junctions and intramembrane particles of astrocytes and oligodendrocytes: a freeze–fracture study. *Neuroscience* **7**, 523–538.

Massa, P. T. & Mugnaini, E. 1985 Cell–cell junctional interactions and characteristic plasma membrane features of cultured rat glial cells. *Neuroscience* **14**, 695–709.

Massa, P. T., Szuchet, S. & Mugnaini, E. 1984 Cell–cell interactions of isolated and cultured oligodendrocytes: formation of linear occluding junctions and expression of peculiar intramembrane particles. *J. Neurosci.* **4**, 3128–3139.

Miller, R. H., Fulton, B. P. & Raff, M. C. 1989 A novel type of glial cell associated with nodes of Ranvier in rat optic nerve. *Eur. J. Neurosci.* **1**, 172–180.

Mobbs, P., Brew, H. & Attwell, D. 1988 A quantitative analysis of glial cell coupling in the retina of the axolotl (*Ambystoma mexicanum*). *Brain Res.* **460**, 235–245.

Moscona, A. A. 1983 On glutamine synthetase, carbonic anhydrase and Müller glia in the retina. *Prog. retinal Res.* **2**, 111–135.

Orkland, R. K. 1977 Glial cells. In *Handbook of physiology. The nervous system. Cellular biology of neurons* (ed J. Brookhardt & V. Mountcastle), vol. 1, pp. 855–875. Washington, D.C.: American Physiological Society.

Rámon-Moliner, E. 1958 A study of neuroglia. The problem of transitional forms. *J. comp. Neurol.* **110**, 157–171.

Ransom, B. R., Butt, A. M. & Black, J. A. 1991 Ultrastructural identification of HRP-injected oligodendrocytes in the intact rat optic nerve. *Glia* **4**, 37–45.

Ransom, B. R. & Kettenmann, H. 1990 Electrical coupling, without dye coupling, between mammalian astrocytes and oligodendrocytes in cell culture. *Glia* **3**, 258–266.

Reichenbach, A., Schippel, K., Schümann, R. & Hagen, E. 1988 Ultrastructure of rabbit retinal nerve fibre layer – neuro-glial relationships, myelination, and nerve fibre spectrum. *Z. Hirnforsch.* **29**, 481–491.

Robinson, S. R. & Dreher, Z. 1989 Evidence for three morphological classes of astrocyte in the adult rabbit retina: functional and developmental implications. *Neurosci. Lett.* **106**, 261–268.

Robinson, S. R., Hampson, E. C. G. M., Munro, M. N. & Vaney, D. I. 1993 Unidirectional coupling of gap junctions between neuroglia. *Science, Wash.* **262**, 1072–1074.

Scherer, J. & Schnitzer, J. 1991 Intraorbital transection of the rabbit optic nerve: consequences for ganglion cells and neuroglia in the retina. *J. comp. Neurol.* **312**, 175–192.

Schnitzer, J. 1985 Distribution and immunoreactivity of glia in the retina of the rabbit. *J. comp. Neurol.* **240**, 128–142.

Schnitzer, J. & Karschin, A. 1986 The shape and distribution of astrocytes in the retina of the adult rabbit. *Cell. Tiss. Res.* **246**, 91–102.

Sontheimer, H., Trotter, J., Schachner, M. & Kettenmann, H. 1989 Channel expression correlates with differentiation stage during the development of oligodendrocytes from their precursor cells in culture. *Neuron* **2**, 1135–1145.

Stone, J. & Dreher, Z. 1987 Relationship between astrocytes, ganglion cells and vasculature of the retina. *J. comp. Neurol.* **255**, 35–49.

Suárez, I. & Raff, M. C. 1989 Subpial and perivascular astrocytes associated with nodes of Ranvier in the rat optic nerve. *J. Neurocytol.* **18**, 577–582.

PHILOSOPHICAL TRANSACTIONS OF THE ROYAL SOCIETY B BIOLOGICAL SCIENCES

Triviño, A., Ramirez, J. M., Ramirez, A. I., Salazar, J. J. & Garcia-Sanchez, J. 1992 Retinal perivascular astroglia: an immunoperoxidase study. *Vision Res.* **32**, 1601–1607.

Vaney, D. I. 1984 'Coronate' amacrine cells in the rabbit retina have the 'starburst' dendritic morphology. *Proc. R. Soc. Lond.* B **220**, 501–508.

Vaney, D. I. 1991 Many diverse types of retinal neurons show tracer coupling when injected with biocytin or neurobiotin. *Neurosci. Lett.* **125**, 187–190.

Vaney, D. I. 1992 Photochromic intensification of diaminobenzidine reaction product in the presence of tetrazolium salts: applications for intracellular labelling and immunohistochemistry. *J. Neurosci. Meth.* **44**, 217–223.

Von Blankenfeld, G., Ransom, B. R. & Kettenmann, H. 1993 Development of cell–cell coupling among cells of the oligodendrocyte lineage. *Glia* **7**, 322–328.

Waxman, S. G. & Black, J. A. 1984 Freeze–fracture ultrastructure of the perinodal astrocyte and associated glial junctions. *Brain Res.* **308**, 77–87.

Wollmann, R. L., Szuchet, S., Barlow, J. & Jerkovic, M. 1981 Ultrastructural changes accompanying the growth of isolated oligodendrocytes. *J. Neurosci. Res.* **6**, 757–769.

Submitted by J. D. Pettigrew; received 22 December 1994; accepted 14 February 1995

PHILOSOPHICAL TRANSACTIONS OF THE ROYAL SOCIETY B BIOLOGICAL SCIENCES

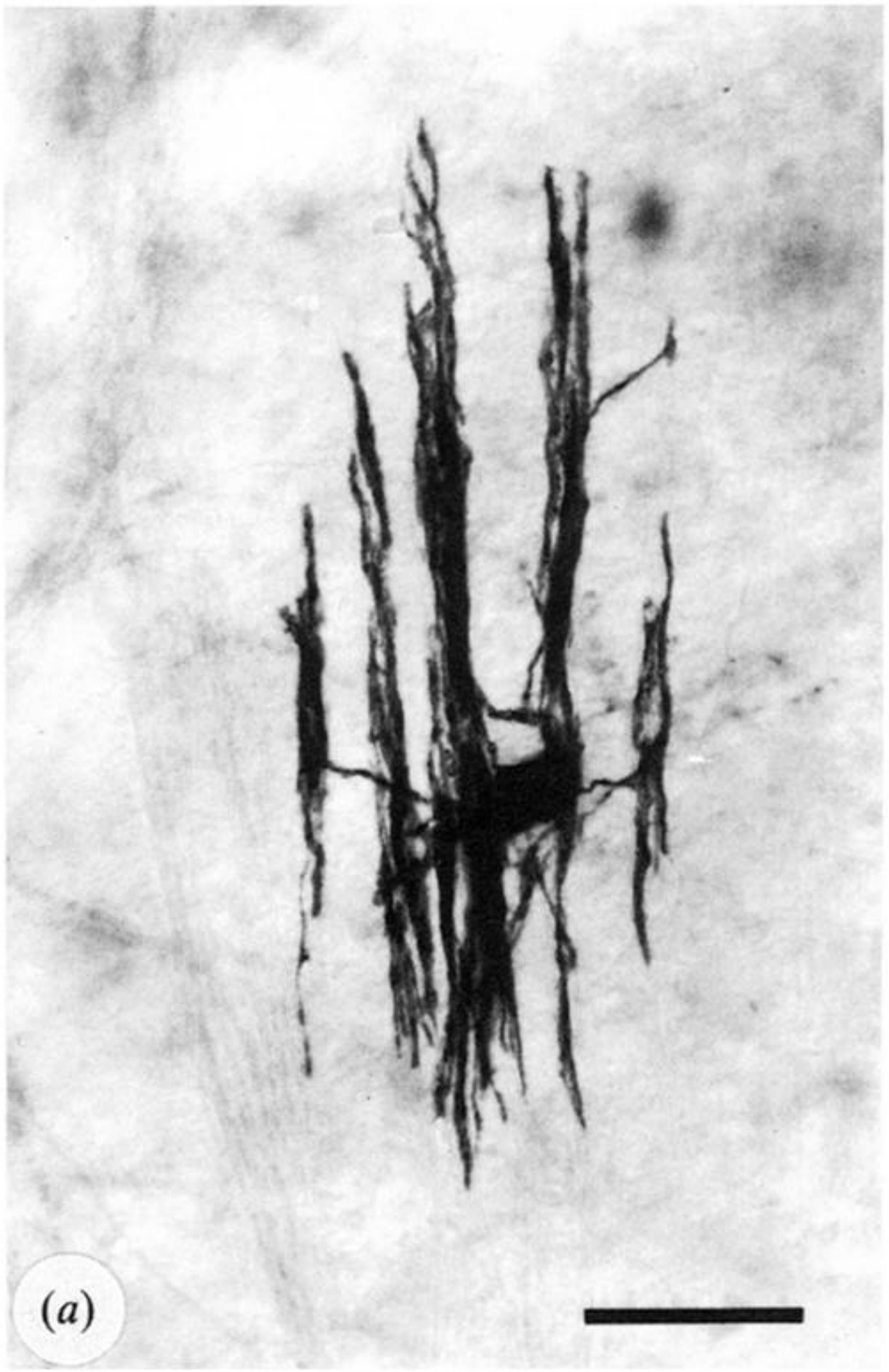

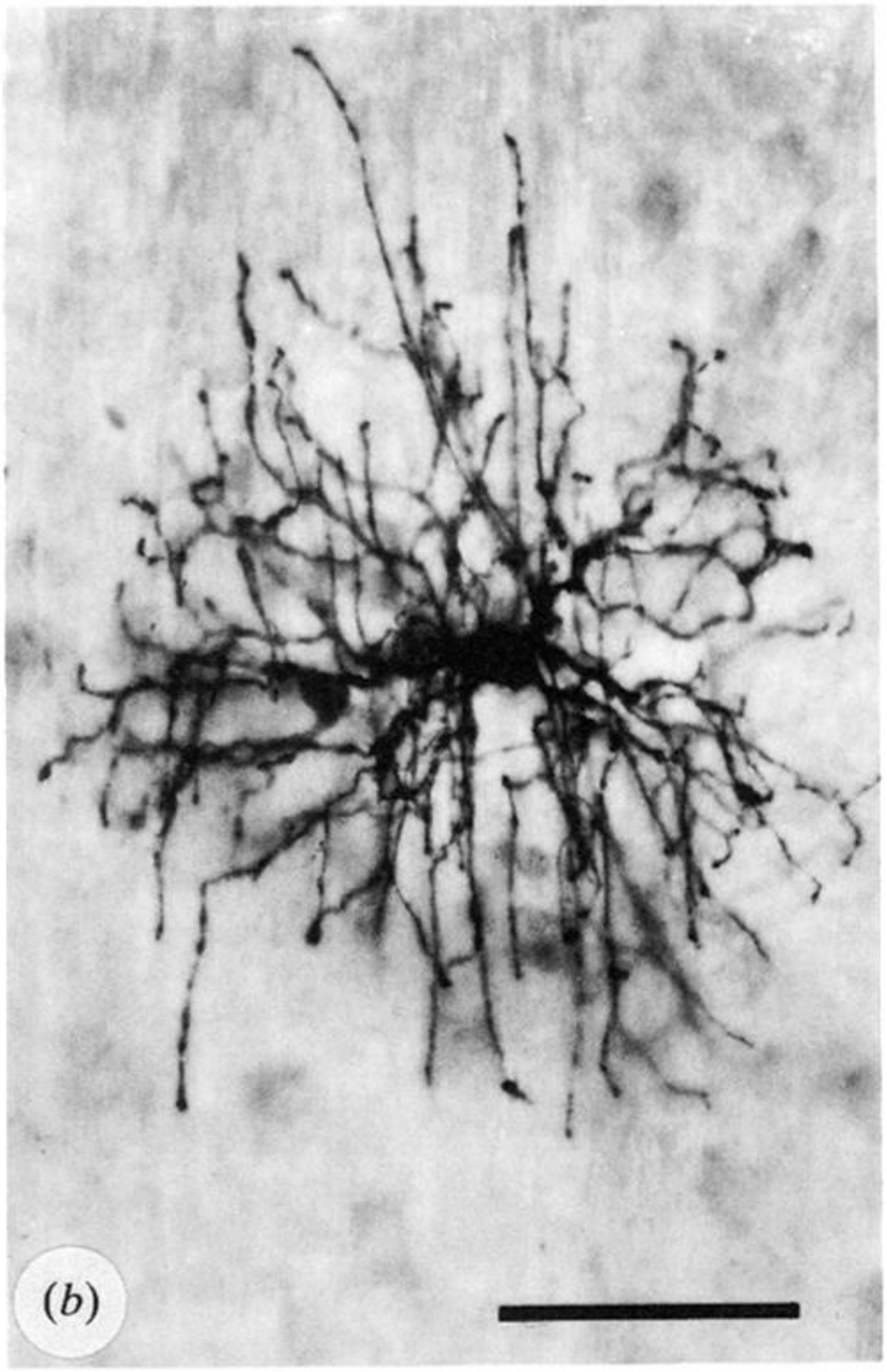

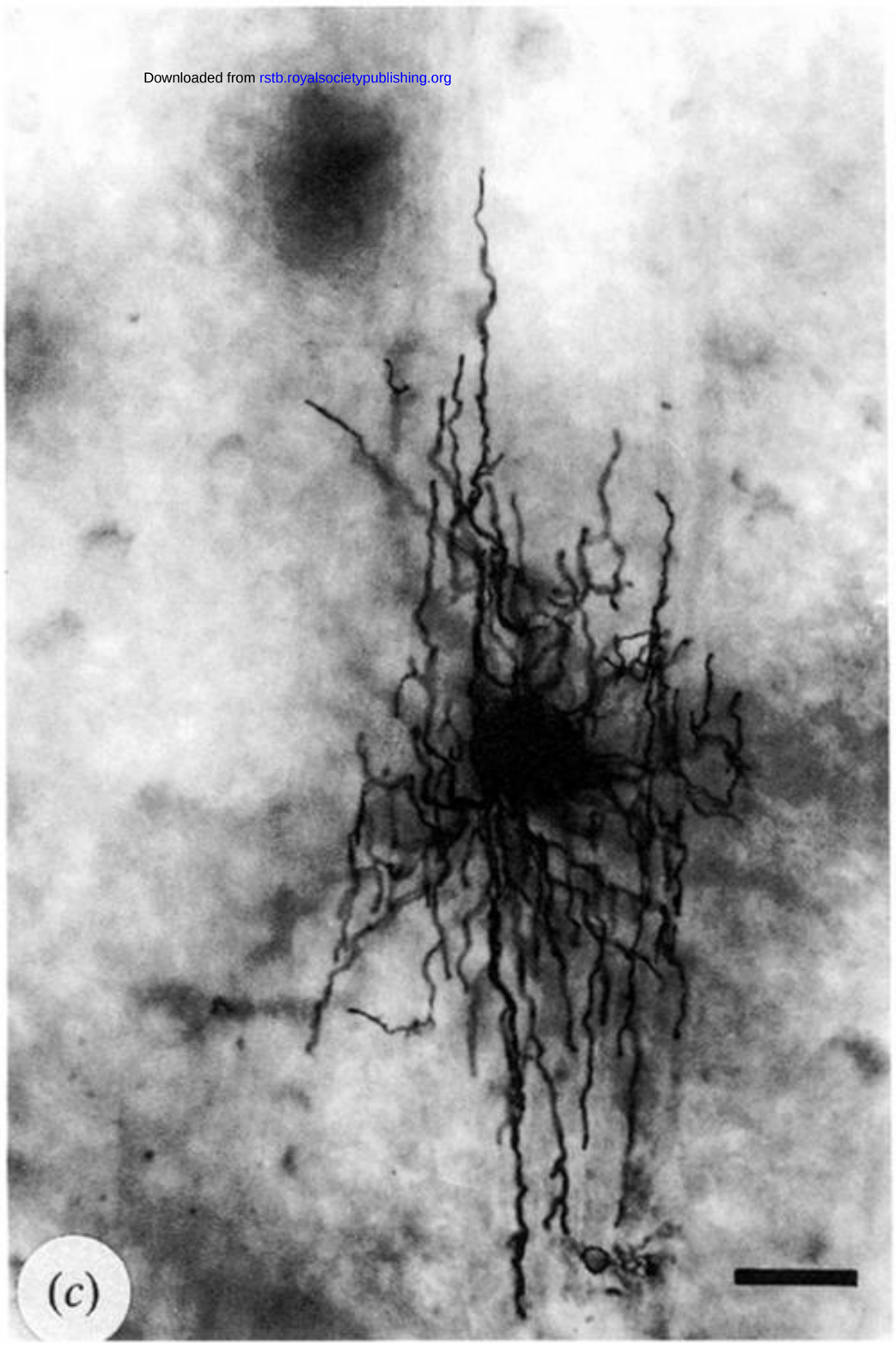

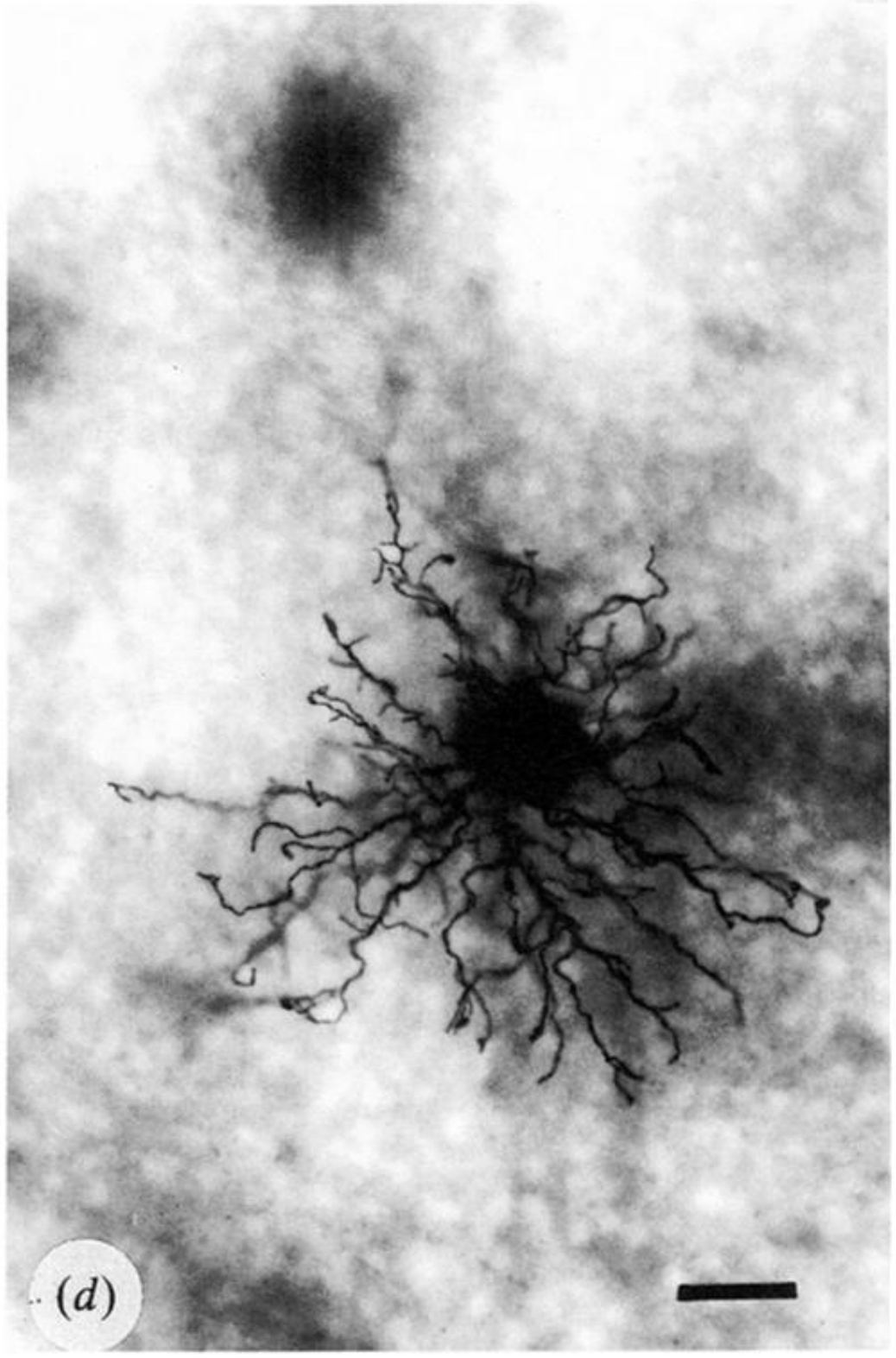

gure 1. Photomicrographs of oligodendrocytes injected with biocytin. (*a*) A parallel oligodendrocyte with processes the NFL. (*b*) A radial oligodendrocyte with processes radiating in all directions within the NFL. (*c*, *d*) A stratified godendrocyte with parallel processes within the NFL (*c*), and deeper radial processes within the IPL (*d*). Scale bars µm.

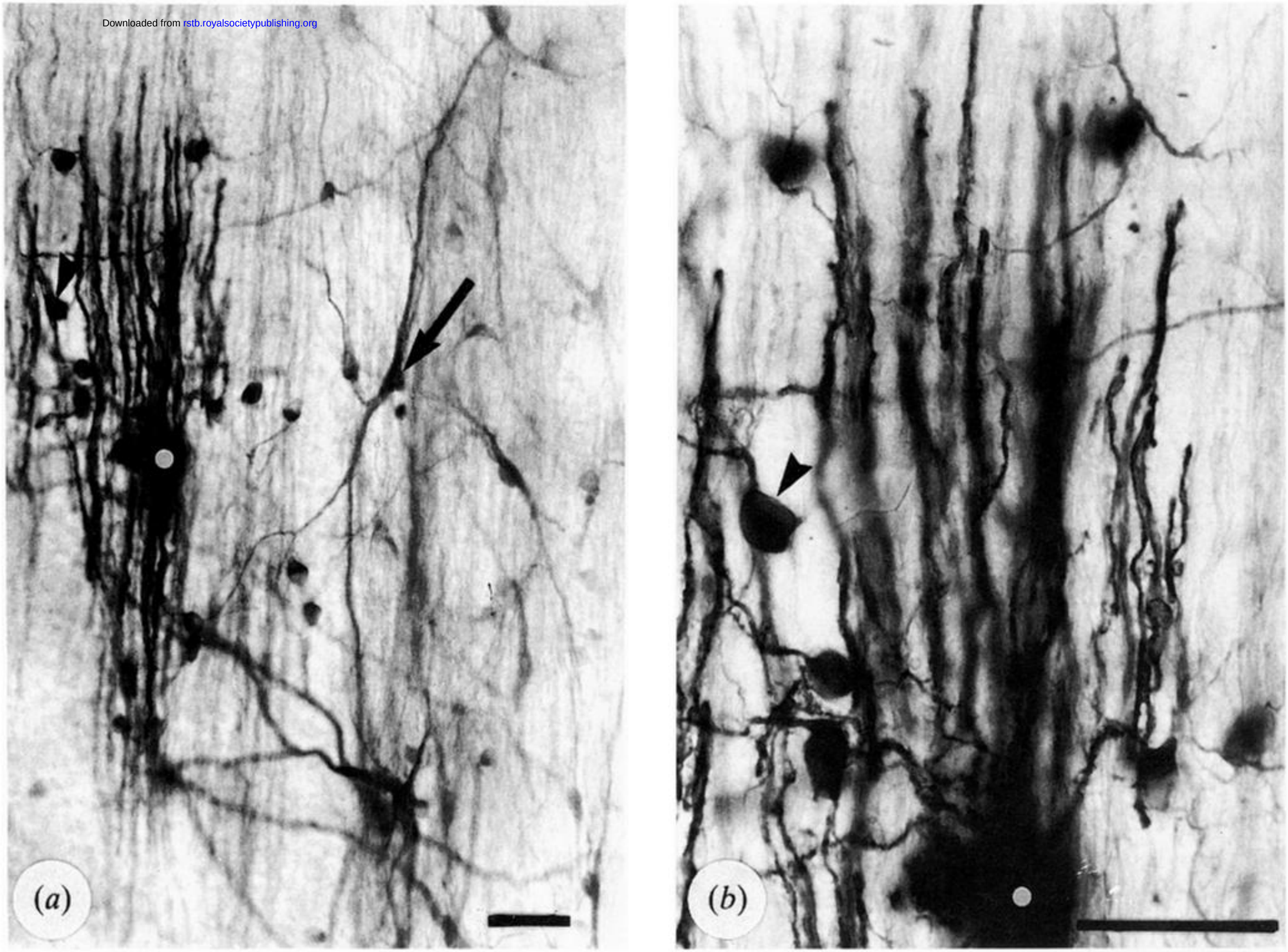

gure 3. Photomicrographs taken at low magnification (*a*) and high magnification (*b*) illustrating the extent of tracer upling between an injected parallel oligodendrocyte (bullseye) and neighbouring oligodendrocytes (arrowhead) d astrocytes (arrow) within the NFL. Scale bars 30 μm.

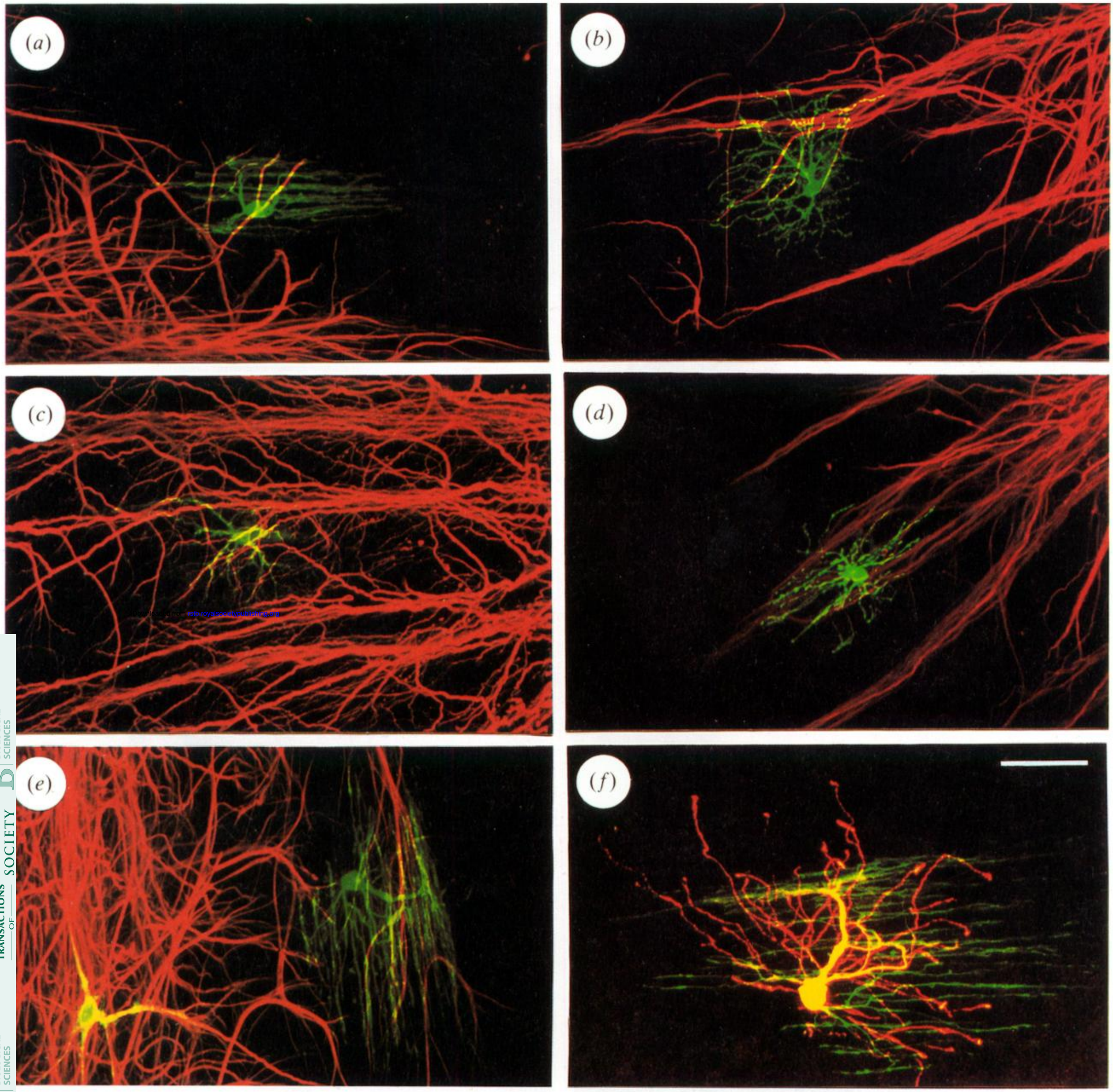

Figure 5. Pseudocolour composite confocal images of oligodendrocytes and astrocytes obtained from a 6 week old rabbit. (*a–e*) Oligodendrocytes injected with Lucifer yellow (green) show morphological heterogeneity, but are not GFAP$^+$, unlike adjacent astrocytes (red). (*a*) A parallel oligodendrocyte with processes in the NFL. (*b*, *c*) Radial oligodendrocytes with processes in the NFL. (*d*) An oligodendrocyte with radiating and parallel processes in the same layer. (*e*) A periaxonal astrocyte injected with Lucifer yellow is also GFAP$^+$ (yellow). A nearby stratified oligodendrocyte (green) is GFAP$^-$. (*f*) Image of the oligodendrocyte injected with Lucifer yellow in (*e*). The cell has been magnified and rotated counterclockwise by 90°. GFAP immunoreactivity is not shown. The superficial, parallel processes of the cell are depicted in green, the intermediate processes are coloured yellow and the deep radial processes are red. Scale bar 50 μm (*a–e*) and 30 μm (*f*).

PHILOSOPHICAL TRANSACTIONS OF THE ROYAL SOCIETY B BIOLOGICAL SCIENCES

igure 6. Photomicrographs of Rip immunoreactivity in retinal oligodendrocytes. (*a*) A presumptive parallel igodendrocyte (asterisk) with fine radial branches (arrowhead) that connect with thicker parallel processes (myelin heaths; arrow) that run parallel to the axons in the NFL. (*b*) A presumptive radial oligodendrocyte with fine recurving rocesses in the NFL. (*c*, *d*) A presumptive stratified oligodendrocyte with processes ramifying in both the NFL (*c*) and he IPL (*d*). Scale bars 30 μm.